PHYSICAL REVIEW B VOLUME 57, NUMBER 11 15 MARCH 1998-I

Magnetic-nonmagnetic transition in fcc 4*d*-transition-metal clusters

R. Guirado-López and D. Spanjaard
Laboratoire de Physique des Solides, Université Paris Sud, F-91405 Orsay, France

M. C. Desjonquères
Commissariat à l'Energie Atomique, DSM/DRECAM/SRSIM, Centre d'Etudes de Saclay, F-91 191 Gif sur Yvette, France

(Received 30 April 1997; revised manuscript received 25 August 1997)

Size-dependent, magnetic, and structural properties of fcc Rh_N and Ru_N clusters ($N=13$, 19, 43, 55, and 79) are calculated using a tight-binding Hubbard Hamiltonian in the unrestricted Hartree-Fock approximation. Results for the magnetic moment, cohesive energy, and interatomic distance at $T=0$ are given as functions of cluster size. The magnetic-nonmagnetic transitions estimated are in agreement with experimental findings. [S0163-1829(98)04308-2]

There has been continuing interest in the intrinsic nature of atomic clusters and how magnetic and structural properties of small clusters evolve into those of the bulk. In particular, transition-metal clusters are of great importance because of their many technological applications in developing magnetic materials with large moments and catalysts with high reactivity.[1,2] Many theoretical calculations[3–7] and measurements[8–10] for 3*d* transition-metal clusters (Fe, Co, and Ni) have indicated that clusters have a larger average magnetic moment per atom than in the bulk phase, and found that the magnetic moments are very sensitive to the local environment.

Among the transition-metal series, the 4*d* series has especially interesting magnetic properties. In the bulk state, all the elements are nonmagnetic; however, theoretical calculations[11] have predicted magnetic ordering in Rh_{13}, Ru_{13}, and Pd_{13} clusters. This fact was confirmed experimentally by Cox *et al.*[12] A wide range of cluster sizes was covered, and the critical size for which the magnetic-nonmagnetic transition is present was estimated.

In the study of magnetic order and structural properties, the bond lengths and the direct atomic neighboring environment are the key quantities. In principle, a determination of both atomic and magnetic properties of transition-metal clusters requires an all-electron computation. However, in the case of Rh and Ru, we have been able to show that a pure *d*-band model can account for these properties.

According to Ref. 13, the cohesive energy (defined negatively) of a transition metal can be expressed as a sum of four contributions:

$$E_{\mathrm{coh}}=E_{\mathrm{prep}}+E_{\mathrm{band}}^{d}+E_{\mathrm{band}}^{sp}+E_{\mathrm{hyb}}^{spd}. \tag{1}$$

E_{prep} is the energy required to prepare a renormalized atom, i.e., an atom in the configuration appropriate to the solid and with wave functions compressed into the Wigner-Seitz sphere of the solid. This term is clearly positive and repulsive. E_{band}^{d} is a negative and attractive term due to the broadening of the renormalized atom *d* level. E_{band}^{sp} is the difference between the average energy of a free-electron band and that of the renormalized atom *s* level. Around bulk equilibrium, this contribution is always negative, and produces a repulsive force which decreases when the number of *d* electrons increases. Finally, E_{hyb}^{spd} is the change of one electron energy due to *sp*-*d* hybridization. This term is negative, almost constant along the series, and produces an attractive force. Therefore, we expect that for some *d*-band filling the forces due to the last two terms cancel. Then the sum of *sp* and *sp*-*d* hybridization contributions can be considered as almost independent of interatomic spacing around equilibrium. The results of Ref. 13 strongly suggest that this could occur for elements in the second half of the series. Assuming that this is actually realized for Rh and Ru, we took *sp*-electron and *sp*-*d* hybridization contributions from Ref. 13 ($E_{\mathrm{band}}^{sp}+E_{\mathrm{hyb}}^{spd}=-2.72$ eV for Rh and $E_{\mathrm{band}}^{sp}+E_{\mathrm{hyb}}^{spd}=-2.4$ eV for Ru), and calculated the *d*-band contribution using the recursion method applied to a tight-binding Hubbard Hamiltonian in the unrestricted Hartree-Fock approximation. This Hamiltonian is the same as the one used previously in Ref. 3. The hopping integrals are deduced from the bulk bandwidth ($W_d=6.3$ eV for Rh, $W_d=7.3$ eV for Ru) using the Andersen law for the distance dependence of the interactions. The on-site energies for spin σ ($\sigma=\pm 1$), $\epsilon_{i\sigma}$, are renormalized by the global charges and magnetic moments as follows:

$$\epsilon_{i\sigma}=\epsilon_{d}^{0}+UN_{d}+U\delta N_{i}-\tfrac{1}{2}\sigma J\mu_{i}, \tag{2}$$

where ϵ_{d}^{0} stands for the bare *d*-level energy of an atom, U is the average direct Coulomb integral ($U=5$ eV for Rh, $U=6$ eV for Ru), and J is the exchange Coulomb integral [$J=0.5$ eV for Rh (Ref. 14), $J=0.44$ eV for Ru (Ref. 15)]. δN_i is given by (N_i-N_d), where N_d is the average number of electrons in the bulk *d* band ($N_d=8$ for Rh, $N_d=7$ for Ru). The local charges (N_i) and the local magnetic moments (μ_i) are determined self-consistently. Finally, E_{prep} can be identified with the repulsive term which is assumed to be pairwise and given by a Born-Mayer potential. The corresponding parameters were obtained from the best fit to the cohesive energy, bulk modulus, and equilibrium distance. The cohesive energy versus distance curve for Rh and Ru within this model is given in Fig. 1 for the bulk structure, and compared to an *ab initio* augmented spherical wave calculation (ASW). The agreement between the two curves is excellent, and

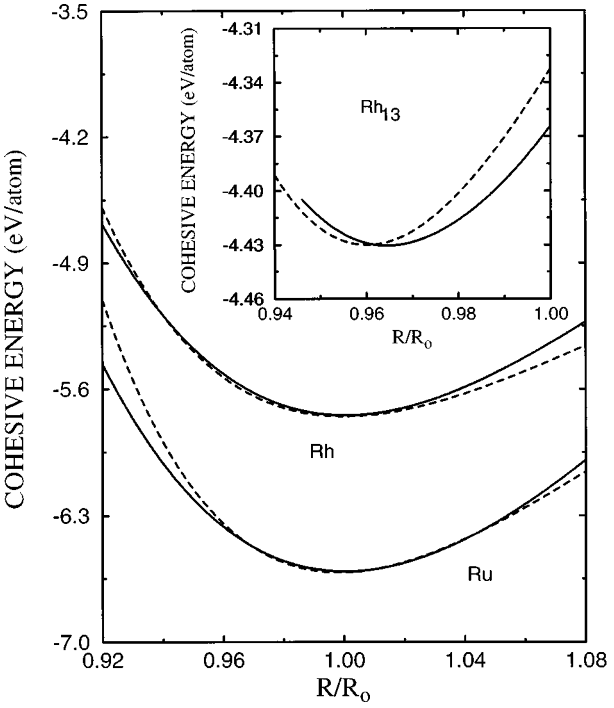

FIG. 1. A comparison of the bulk cohesive energy for fcc rhodium and ruthenium as a function of the interatomic distance. The solid line refers to an *ab initio* (ASW) calculation and the dashed line to our tight-binding calculation. In the inset, a comparison of the cohesive energy per atom for the fcc Rh_{13} cluster as a function of the interatomic distance. The solid line refers to an ab initio calculation (DMOL), and the dashed line to our tight-binding result. Our calculated tight-binding energies were shifted rigidly by 1.98 eV in order to match, at the equilibrium distance, the cohesive energy of the DMOL calculation.

proves that the variation with the distance of $E^{sp}_{\mathrm{band}}+E^{spd}_{\mathrm{hyb}}$ can be neglected for these elements. We have also checked that this assumption remains valid for clusters, by comparing in the inset of Fig. 1 our results for Rh_{13} with an *ab initio* calculation using the DMOL program.[16] The agreement between both results justifies this assumption and the transferability of the tight-binding parameters.

The determination of the geometrical arrangement of the atoms is one of the main difficulties in a theoretical study of free clusters, since direct experimental information about the cluster structure is very difficult to obtain. Nevertheless, we will be able to analyze roughly the behavior of the magnetic moment with the number N of atoms in the cluster and we will try to predict the value N_c for which we have the magnetic-nonmagnetic transition, by considering a fcc growth, i.e., by adding to a central atom the shells of first ($N=13$), second ($N=19$), third ($N=43$), fourth ($N=55$), and fifth nearest neighbors ($N=79$).

For each size, we performed a uniform relaxation, minimized the energy with respect to the distance, and obtained the equilibrium bond-length $R_0(N)$, the d part of the cohesive energy $E^d_{\mathrm{coh}}(N)=E_{\mathrm{prep}}(N)+E^d_{\mathrm{band}}(N)$, and the magnetic moment.

In Table I, we report the calculated magnetic moments in Rh_N clusters for each type of site in the structures, the moment on atoms in the jth shell of neighbors of the central atom (shell 1) being denoted as $\mu(j)$. For the Rh_{13} cluster, we can see that the surface atoms have larger magnetic moments, since the local coordination is smaller and the degree of localization is greater.

Ferromagnetic order is obtained for the Rh_{13}, Rh_{19}, and Rh_{43} clusters. For Rh_{55} we obtain two antiferromagnetic self-consistent solutions with the same configuration $(\uparrow\downarrow\downarrow\downarrow\downarrow)$. The difference in energy for the two solutions is $\Delta E_{\mathrm{coh}}(55)=E^{(a)}_{\mathrm{coh}}(55)-E^{(b)}_{\mathrm{coh}}(55)=0.002$ eV, a value which is too small to conclude safely, taking into account the approximations we made, about the most stable solution. However, note that the magnitude of $\langle\mu^{(a)}\rangle$(the most stable solution in our model) is located within the experimental error.[12] An antiferromagnetic configuration is also obtained for $Rh_{79}(\uparrow\uparrow\downarrow\downarrow\downarrow\downarrow)$.

In the $Rh^{(a)}_{55}$ and Rh_{79} clusters, we note that the magnetic moment of the central atom has almost vanished, as in the bulk. This is in agreement with previous transition-metal calculations,[17] which proved that if the central atom in the cluster is surrounded by three or more nearest-neighbor shells it will have bulklike properties. However, it is important to note that the convergency of the magnetic moment to the bulk value is smoother on the second shell $[\mu(2)]$ than on the central atom. This is due to the fact that the perturbation introduced by the surface of the cluster is symmetric around the atom in the center, and therefore produces very strong changes in its local density of states, causing strong oscillations in the value of $\mu(1)$. These oscillations can be interpreted as indicating how deep the perturbation caused by the surface penetrates into the cluster.

The effect of relaxation in the magnetic moments produces changes as large as 50%; for example, in the unrelaxed 13-atom cluster we have $\langle\mu\rangle=1.57\mu_B$/atom, and for the relaxed one we obtain $\langle\mu\rangle=0.77\mu_B$/atom. In Fig. 2, we can see the behavior of the magnetic moment with cluster size for relaxed and unrelaxed structures compared with the ex-

TABLE I. The calculated local magnetic moments $\mu(j)$ on successive neighbor shells around the central atom ($j=1$) and average magnetic moments $\langle\mu\rangle$ (in units of μ_B) for the relaxed structures in fcc rhodium clusters.

Cluster	$\mu(1)$	$\mu(2)$	$\mu(3)$	$\mu(4)$	$\mu(5)$	$\mu(6)$	$\langle\mu\rangle$
Rh_{13}	0.250	0.815					0.77
Rh_{19}	1.172	1.076	0.644				0.94
Rh_{43}	0.511	0.260	0.023	0.400			0.31
$Rh^{(a)}_{55}$	−0.096	0.216	0.034	0.174	0.218		0.17
$Rh^{(b)}_{55}$	−0.340	0.189	0.153	0.595	0.647		0.45
Rh_{79}	−0.019	−0.007	0.077	0.001	0.044	0.146	0.05

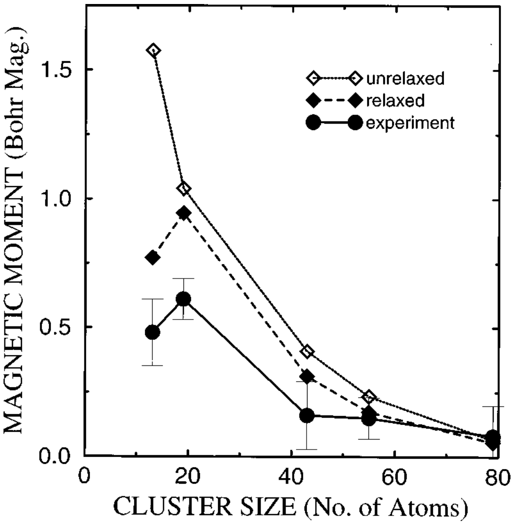

FIG. 2. A comparison of the calculated average magnetic moments for relaxed and unrelaxed structures of Rh clusters, with the experimental measurements as a function of the number of atoms in the cluster.

perimental results. As expected, for the larger clusters in which the contraction of the distance is smaller, the unrelaxed and relaxed calculations are very close. Note that the values of the magnetic moments in the relaxed structures follow the same trends as the experimental ones, and that a nonmonotonic size dependence is observed. A high value of $\langle\mu\rangle$ for $N=19$ with respect to the neighboring clusters is obtained, in agreement with experiment, while other calculations always predict a decreasing behavior for $\langle\mu\rangle$ when the size increases. As we can see, for small clusters our calculated magnetic moments are larger than the experimental ones, which may suggest that for these sizes it is necessary to consider more complicated structures. However, for the larger clusters, our results are very close to the experimental measurements, which could be an indication that for $N>40$, fcc structures are preferred.

A reduction in the interatomic distance is found for all the aggregates, in agreement with previous calculations for transition-metal clusters. The maximum deviation (compared to the bulk interatomic distance) is a contraction of 4% in the 13-atom cluster, which is almost equal to the one calculated with first-principles methods.[18]

Results for Ru_N clusters are shown in Table II. As we can see, the average magnetic moment per atom obtained for the Ru_{13} cluster is much smaller than the one obtained by Reddy, Khanna, and Dunlap ($1.07\mu_B$/atom),[11] but in good agreement with the experimental upper limit of $0.29\mu_B$/atom.[12] Our calculated magnetic moment is also small compared to the value obtained for the same cluster with an *ab initio* calculation by Kaiming *et al.*,[19] and which is equal to the one given in Ref. 11. As in the Rh_{13} case, we observe that surface atoms have larger magnetic moments due to the reduced coordination number. For Ru_{19}, we have an almost zero value for $\langle\mu\rangle$, and, contrary to Rh_{19}, the magnetic moment of the central atom is very small, which means that in this case the perturbation caused by the second shell of neighbors does not go too deep into the cluster. However, we can see that small oscillations are present in $\mu(1)$ when the size of the clusters increases.

The values obtained for the magnetic moments for the Ru_{19}, Ru_{43}, and Ru_{55} clusters by Kaiming *et al.*[19] are higher than the ones calculated in this work, as we can see in Table II. However, the influence of relaxation in the structures for $N=19$, 43, and 55 was not considered in this *ab initio* calculation.

Antiferromagnetic solutions were found for all the Ru_N clusters with the following configurations: Ru_{13}:$\downarrow\uparrow$, Ru_{19}:$\uparrow\uparrow\downarrow$ and Ru_{43}:$\uparrow\downarrow\uparrow\uparrow$. Similar arrangements have been found in fcc iron clusters, which, maybe, shows some correlation in the magnetic properties between isoelectronic elements of the transition-metal series.

Considering absolute values of the average magnetic moment smaller than $0.1\mu_B$/atom to be of the order of the experimental error, we can estimate the magnetic-nonmagnetic transition to be located between $13<N_c<19$, while in Ref. 19 we can find significant values for the average magnetic moment in the Ru_{55} cluster. This value of N_c is very similar to the value $N_c=11$, estimated for Ru_N clusters using a tight-binding Friedel model,[20] and is also in agreement with the experimental result[12] that estimates the transition for $N\geqslant 12$.

A reduction in the interatomic distance was found for all the clusters. In Ru_{13}, we obtain a maximum contraction of approximately 5%, which is larger than the one obtained in the local-spin-density calculation (3.16%).[19] Contrary to the Rh_{13} cluster, we found that the average magnetic moment in Ru_{13} (as for the other sizes) is not very sensitive to changes in the interatomic distance. However, for both Rh_N and Ru_N clusters, the local magnetic moments $\mu(j)$ are sensitive to changes in the cluster size (see Tables I and II) and in the interatomic spacing.

The quantity $E_{\mathrm{coh}}^{d}(N)$cannot be directly compared to the cohesive energy per atom, since it does not include the contributions of the sp electrons and sp-d hybridization. We have shown that this contribution for a given structure is fairly insensitive to distance variations around equilibrium; however, it is expected to depend on the average coordination number z_{eff}. We have found that if this contribution scales as $(z_{\mathrm{eff}})^{1/2}$, the cohesive energy per atom is in fair agreement with *ab initio* calculations, as we can see in Table

TABLE II. Same caption as Table I for fcc ruthenium clusters. For comparison, the results for $\langle\mu\rangle$ obtained in Ref. 19 are also given.

Cluster	$\mu(1)$	$\mu(2)$	$\mu(3)$	$\mu(4)$	$\mu(5)$	$\langle\mu\rangle$	Ref. 19
Ru_{13}	-0.080	0.244				0.219	1.07
Ru_{19}	0.001	0.068	-0.031			0.033	0.42
Ru_{43}	0.025	-0.005	0.012	0.049		0.028	0.13
Ru_{55}	0.000	0.000	0.000	0.000	0.000	0.000	0.10

TABLE III. The cohesive energy per atom calculated using our model compared with *ab initio* results (see Ref. 19) for Ru clusters.

Cluster	$\lvert E_{\mathrm{coh}}(N)\rvert$ (eV/atom)	Ref. 19
Ru_{13}	5.37	5.20
Ru_{19}	5.57	5.66
Ru_{43}	5.81	6.17
Ru_{55}	6.00	6.56
$\mathrm{Ru}_{\mathrm{bulk}}$	6.61 (Ref. 21)	6.74

III for Ru clusters. Note that, in the last calculation, the evolution of the cohesive energy per atom as N increases converges to the bulk value faster than in ours. However if we compare the excess energy per surface atom in both calculations for $N=55$, we find that *ab initio* results give ~0.24 eV, while our model leads to ~0.8 eV. This last value seems more reasonable when compared to surface energies.

In this paper, we reported a comprehensive study of the electronic properties and magnetism of fcc Rh_N and Ru_N clusters, by using a tight-binding Hubbard Hamiltonian for the d band in the unrestricted Hartree-Fock approximation. We showed that this model is able to predict magnetic properties and atomic relaxations reliably for these two elements. The local magnetic moments and magnetic ordering were studied at $T=0$. Our results are consistent with a fcc growth in rhodium clusters for $N>40$, and we estimate the magnetic-nonmagnetic transition to be located at $N_c \approx 80$. For fcc Ru_N clusters, the value of the critical size N_c is considered to be located between $N=13$ and 19. Ferromagnetic order was present in Rh_N clusters with $N=13$, 19, and 43, and, for larger sizes, we obtained antiferromagnetic configurations. In the Ru_N clusters, only antiferromagnetic configurations were obtained for the relaxed structures. Bond-length contractions, as compared to the bulk interatomic spacing, were found in all the optimized structures in agreement with *ab initio* calculations. Finally, a simple assumption made on the variation of the sp and sp-d hybridization contributions allowed us to derive reasonable values of the cohesive energy per atom in the clusters.

R.G.-L. would like to acknowledge financial support by CONACyT (México), the hospitality of the Service de Recherche sur les Surfaces et l'Irradiation de la Matière of the CEA de Saclay, and Professor J. Dorantes-Dávila, who introduced him to the electronic structure calculations. Finally, we thank Dr. C. Coudray and Dr. C. Barreteau for helpful discussions.

---

[1] E. P. Wohlfarth, Phys. Status Solidi A **91**, 339 (1985).

[2] M. R. Zapkin, D. M. Cox, R. O. Brickman, and A. J. Kaldor, J. Phys. Chem. **93**, 6823 (1989).

[3] G. M. Pastor, J. Dorantes-Dávila, and K. H. Bennemann, Phys. Rev. B **40**, 7642 (1989).

[4] F. Liu, S. N. Khanna, and P. Jena, Phys. Rev. B **43**, 8179 (1991).

[5] K. Lee, J. Callaway, and S. Dhar, Phys. Rev. B **30**, 1724 (1985).

[6] K. Lee and J. Callaway, Phys. Rev. B **48**, 15 358 (1993).

[7] Z. Q. Li and B. L. Gu, Phys. Rev. B **47**, 13 611 (1993).

[8] W. A. deHeer, P. Milani, and A. Chatelain, Phys. Rev. Lett. **65**, 488 (1990).

[9] D. C. Douglass, J. P. Bucher, and L. A. Bloomfield, Phys. Rev. B **45**, 6341 (1992).

[10] J. G. Louderback, A. J. Cox, L. J. Lising, D. C. Douglas, and L. A. Bloomfield, Z. Phys. D **26**, 301 (1993).

[11] B. V. Reddy, S. N. Khanna, and B. I. Dunlap, Phys. Rev. Lett. **70**, 3323 (1994).

[12] A. J. Cox, J. G. Louderback, S. E. Apsel, and L. A. Bloomfield, Phys. Rev. B **49**, 12 295 (1994).

[13] C. D. Gelatt, Jr., M. Ehrenreich, and R. E. Watson, Phys. Rev. B **15**, 1613 (1977).

[14] A. Chouairi, H. Dreyssé, H. Nait-Laziz, and C. Demangeat, Phys. Rev. B **48**, 7735 (1993).

[15] B. Piveteau, M. C. Desjonquères, A. M. Oleś, and D. Spanjaard Phys. Rev. B **53**, 9251 (1996).

[16] B. Delley, J. Chem. Phys. **92**, 508 (1990); **94**, 7245 (1991).

[17] M. R. Press, F. Liu, S. N. Khanna, and P. Jena, Phys. Rev. B **40**, 399 (1989).

[18] Y. Jinlong, F. Toigo, W. Kelin, and Z. Manhong, Phys. Rev. B **50**, 7173 (1994).

[19] D. Kaiming, Y. Jinlong, X. Chuamyun, and W. Kelin, Phys. Rev. B **54**, 2191 (1996).

[20] J. Zhao, X. Chen, Q. Sun, F. Liu, and G. Wang, Europhys. Lett. **32**, 113 (1995).

[21] C. Kittel, *Introduction to Solid State Physics*, 5th ed. (Wiley, New York, 1976).